GRADIENT STAINLESS STEEL BUFFER LAYER TO SUPPORT ALUMINIUM NITRIDE DIFFUSION BARRIER FOR CARBON NANOTUBES GROWTH

PANTOJA-SUAREZ Fernando[1,2,3], ALSHAIKH Islam[1,2], AMADE Roger[1,2], ANDUJAR José-Luis[1,2], PASCUAL Esther[1,2], BERTRAN-SERRA Enric[1,2]

[1]FEMAN Group, Dep. Applied Physics, Barcelona University, Barcelona, Spain, EU
[2]Institute of Nanoscience and Nanotechnology (IN2UB), Barcelona University, Spain, EU
[3]Department of Materials, Faculty of Mechanical Engineering, National Polytechnic School, Ladrón de Guevara, Quito, Ecuador

Abstract

We propose a new effective method to keep the catalyst nanoparticles on the surface of bulk stainless steel 304 (SS304) to grow carbon nanotubes (CNTs). This method consists on the creation of a buffer layer of nitrided stainless steel and a top barrier layer of aluminium nitride (AlN). For that, we have followed two steps. A first step consists on a DC-pulsed reactive sputtering process from SS304 target and a second step of reactive sputtering from aluminium target. Stainless steel nitrided layer (G-SS304) was produced by increasing the nitrogen concentration in the Ar atmosphere in order to obtain a gradient buffer layer on SS304. On the other hand, the AlN layer was produced by a fixed nitrogen concentration in the argon atmosphere. The catalyst nanoparticles were performed on top of the multilayer system after the deposition of an ultrathin Fe layer, which transforms in a monolayer of isolated Fe nanoparticles acting as catalyst during CNTs growth. The aim of this study is to present an alternative methodology for producing CNTs grown on stainless steel. We used different temperatures to obtain CNTs: 680, 700, 715 and 730 °C. Scanning electron microscope (SEM) images showed the influence of temperature over the performance of this new configuration. Raman characterization provided structural information about the CNTs. One of the applications of this method is the production of high specific surface electrodes based on stainless steel for electrochemical devices.

Keywords: Gradient stainless steel, buffer layer, aluminium nitride, carbon nanotubes

1. INTRODUCTION

Nowadays, stainless steel is one of the metallic alloys with a major variety of applications in different productive and research fields. The main applications are in the fields like petrochemical, transport, food, conductors, storage and energy [1-6]. The surface modification of this versatile material has different purposes, such as increase of corrosion resistance and hardness, reducing wear rates [1,2], controlling the wettability behavior [3] and allowing the growth of nanostructures [4-5]. Physical, chemical, mechanical and thermal processes have been used for tuning its surface properties. Modern trends of surface modification include a plasma-based surface treatment. One of the most widespread technologies used in the industry is the magnetron sputtering. It allows the deposition of a great variety of metallic, non-metallic, alloys and compounds. Some researchers have studied mechanical coatings of stainless steel deposited by this technique [6-10]. In particular, Saker et al. [6] found high nitrogen supersaturation of austenite in the stainless-steel layers obtained by sputtering, which presented a rather low compressive stress and a high value of micro hardness. Surface modification allows interesting uses of stainless steel, for example as a substrate to grow nanostructures or even to act as a diffusion barrier. Romero et al. [5] modified the native chromium oxide of stainless steel to grow carbon nanotubes (CNTs). In this case, the oxidized layer acted as a diffusion barrier. The rich phases of iron, nickel and chromium on the surface acts as a catalyst to obtain CNTs although there is a considerable amount of amorphous carbon. Other alternatives permit to obtain CNTs forest on stainless steel with low percentage of amorphous carbon, as an example, using a buffer layer along with a diffusion barrier [4]. These

diffusion barriers are usually based on thin layers of Al_2O_3, TiN, TiO_2, AlN, avoid the diffusion of catalyst inside of bulk stainless steel. In order to circumvent the effects of thermal stress an effective buffer layer can be used. Thus, pure Al, Ti, Cr, Ni buffer monolayers and multilayers avoid the formation of cracks in the diffusion barrier surface during thermal process in order to prevent the contamination of catalyst particles [11,12]. The synthetized process of CNTs directly on this conductive substrate, instead of the conventionally silicon wafer, improves the device performance, makes unnecessary the transfer step of CNTs, prevents the use of any additional material that may increase the total mass of the electrode, and offers a lower contact resistance that improves the electron/thermal transport properties [13].

The aim of this study is to present an alternative methodology for producing CNTs grown on stainless steel in a simplified way to obtain similar or better results than the described above. This new methodology is based in a direct and gradual nitruration of the buffer layer deposited by reactive sputtering from a stainless-steel target. This gradient nitrided buffer layer has no abrupt interfaces with the bulk material. We have evaluated the efficiency of the gradient stainless steel 304 (G-SS304) buffer layer deposited on bulk stainless steel 304 (SS304) combined with a thin layer of aluminium nitride (AlN) acting as a barrier to avoid the dissolution of Fe into the SS304 substrate. For this study, high purity iron nanoparticles have been used as a catalyst material. Different temperatures were used to obtain forest of CNTs. The morphology and the quality of the system CNTs/AlN/G-SS304/SS304 were studied using Scanning Electron Microscope (SEM) and Raman spectroscopy.

2. EXPERIMENTAL PROCEDURE

2.1. Preparation of substrate surface SS304 and deposition process of G-SS304/AlN films

AlN/G-SS304 coatings were deposited on SS304 substrate foil of 0.1 mm thickness. Before deposition, the substrates were cleaned with acetone and isopropanol in an ultrasonic bath for 10 minutes, respectively. The diffusion barrier system (AlN/G-SS304) was deposited using a multifunctional reactor that combines plasma enhanced chemical vapor deposition (PECVD) and magnetron sputtering. A SS304 substrate foil of 0.1 mm thickness and 9 cm^2 of area was fixed on the substrate holder, 8 cm away in front of the sputtering header and cleaned using Ar plasma to etch the native oxide film. **Figure 1** shows the configuration of the system that we used. The diffusion barrier was deposited by two steps. Firstly, a gradient layer of nitrided steel (G-SS304) was deposited on bulk SS304 substrate by DC-pulsed sputter process (50 W, 100 kHz, duty-cycle 2016 ns) using a SS304 target. The sputtering process started with 20 sccm Ar flowing during 600 s. Progressively, N_2 was introduced and Ar was reduced during 100 s until reaching 3/17 sccm flow of N_2/Ar. This regime was kept during 500 s. During 100 s, the N_2/Ar flow was changed again until reaching 7/13 sccm then it was kept during 500 s. The deposition process was carried out at 1 Pa of total pressure and at room temperature. Secondly, a 10 nm aluminum nitride (AlN) thin layer was deposited on top of the nitrided steel gradient layer using DC-pulsed sputtering (120 W, 100 kHz, duty-cycle 2016 ns) with an Al target with 20/30 sccm N_2/Ar flowing and 3 Pa of total pressure at room temperature.

2.2. Nucleation and carbon nanotubes growth

The substrate, with the diffusion barrier system, was transferred to a CNTs reactor. In this reactor, a 2.5 nm layer of catalyst material was deposited on this substrate using RF sputtering process from a high purity Fe target (3 inches of diameter) using Ar. The technological parameters for iron layer were: 2 Pa of Ar (flow rate 128 sccm) and 50 W of RF power (13.56 MHz). Then, the sample was placed under a heating element in order to anneal the catalyst layer and grow the CNTs.

The CNTs growth process was carried out by two steps: (a) annealing during 870 s (750 s ramp time and 120 s hold time) under H_2 (100 sccm, 200 Pa), hold time is necessary to allow the formation of iron nanoparticles and (b) during 30 s, H_2 was purged and the NH_3 was introduced (100 sccm, 80 Pa). Then,

plasma (50 W of RF power) was ignited and 100 sccm of the gas precursor (C_2H_2) was introduced [13,14]. The total pressure of the gas mixture was set pointed to 100 Pa. The CNTs growth was carried out for a total time of 900 s. We used different annealing temperatures to obtain CNTs: 680, 700, 715 and 730 °C.

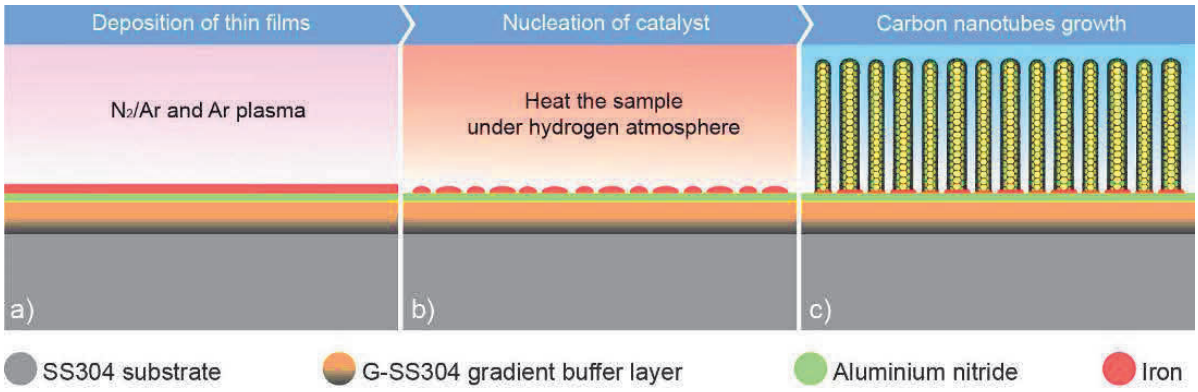

Figure 1 Transversal section of the gradient stainless steel buffer layer supporting the aluminium nitride layer, the catalyst Fe nanoparticles and the CNTs. a) before annealing process, b) after annealing process and c) with CNTs forest

2.3. Characterization techniques

The morphology of the samples was determined by scanning electron microscopy (SEM) (Jeol JSM-6510), equipped with an energy dispersive X-ray (EDX) detector. The Raman spectroscopy (HORIBA LabRam HR800, Japan) provided the effect of the growth temperature on the quality of CNTs. A green laser of 532 nm wavelength and 0.5 mW power using a 100 objective were used during the measurements.

3. RESULTS AND DISCUSSION

3.1. Deposition rate of AlN and G-SS304

To determine the deposition rate, we used a glass substrate and profilometry measurements using a KLA Tencor, D-120. **Table 1** contains the list of the deposition rate values of each layer. For AlN layer the deposition rate was 0.03 $nm \cdot s^{-1}$. Using a Box-Wilson experimental design, we found that the a N_2/Ar flow ratio of 20 / 30 sccm allows us to obtain a uniform AlN layer that acts as an effective diffusion barrier for Fe nanoislands. AlN is a low-cost alternative to support catalyst materials [15].

The measured values of the deposition rate of G-SS304 layers decreases with the increase of the N_2/Ar flow ratio. This change can be explained by the loss of efficiency associated to the decrease of Ar concentration during the sputtering process. In addition, when the N_2 percentage increases, it induces continued poisoning of the target [10].

Table 1 Deposition rate for AlN and G-SS304

Layer	Flow ratio N_2/Ar (sccm)	Deposition rate ($nm \cdot s^{-1}$)
Aluminium nitride	20 / 30	0.03
G-SS304	7 / 13	0.10
	3 / 17	0.11
	0 / 20	0.13

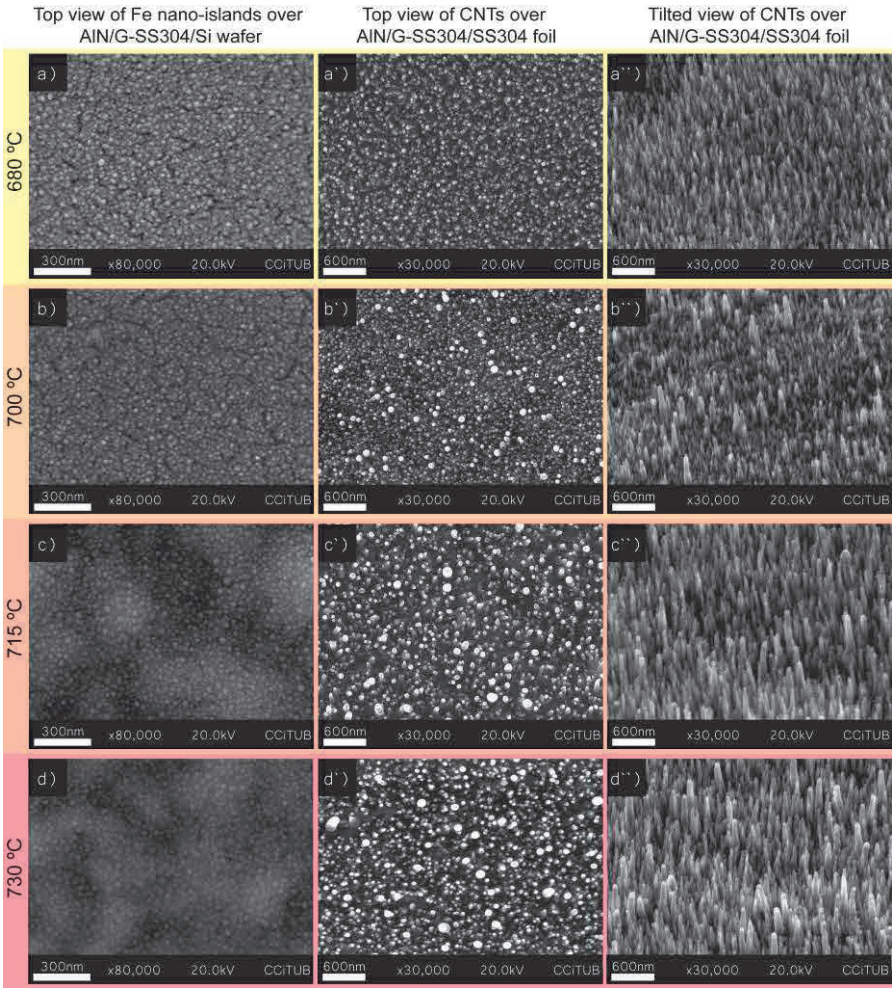

Figure 2 SEM images of Fe nanoislands and CNTs forest obtained at different temperatures. *a, b, c* and *d* correspond of top view of Fe nanoislands on AlN/G-SS304/Si wafer. *a`, b`, c` and d`* show the top view of CNTs on AlN/G-SS304/SS304. *a``, b``, c`` and d``* show the tilted view of CNTs on AlN/G-SS304/SS304

3.2. Morphological characterization

In order to study the nucleation of catalyst on AlN/G-SS304, Si wafers were used as a substrate. Polished Si wafers were used instead of stainless steel because it is difficult to observe the nanoislands on SS304 with a roughness of tens of microns. SEM images **(Figures *2a, 2b, 2c*** and ***2d*)** show a uniform distribution of nanoislands. Using ImageJ software, the density for different temperatures was determined. The obtained values are 1.67 x 10^9, 1.33 x 10^9, 1.27 x 10^9 and 1.08 x 10^9 nanoislands/mm^2 for 680, 700, 715 and 730 ºC, respectively. The density decreases when the annealing temperature increases. Also, the average of diameter increases from 12 to 20 nm at high temperatures. This is because the particles of Fe at high temperatures start the coalescence [16]. Additionally, there were cracks on these samples, which were produced during the annealing process due to the difference between the thermal expansion coefficient of Si and AlN/G-SS304 layer. The densities of CNTs on SS304 foil (**Figures *2a`, 2b`, 2c`*** and ***2d`***) are lower than the value obtained for Fe particles. The kinetic processes that occur in each system (Fe/AlN/G-SS304/Si wafer and Fe/AlN/G-SS304/SS304 foil) are different [11]. In a future work, we will study the diffusion processes that occur in these systems to optimize the thickness of each layer. The most homogeneous forest of CNTs was obtained at 680 °C (**Figures*2a`, 2a``***). The average length of CNTs is 500 nm. Additionally, the diameter was between 20-25 nm. At 730 °C (**Figures 2d`*, 2d``***) the CNTs forest shows a random morphology with diameters ranging from 30 to 70 nm and lengths between 600-1000 nm. The CNTs obtained at 730 ºC are longer than the others

CNTs obtained at lower temperatures. However, the high temperature produces coalescence of catalyst nanoislands. The average diameter of these particles is bigger than the particles obtained at 680 ºC. Also, **Figures 2*b*`** and **2*b*``** show a mixed forest of CNTs. High percentage of these CNTs are similar to the CNTs obtained at 680 ºC. **Figures 2c`** and **2c``** also show a mixed forest of CNTs. Nevertheless, a low percentage of these CNTs obtained are similar to those obtained at 680 ºC. This sequence of images shows the strong influence of temperature during carbon nanotube growth. Grüneis et al. demonstrate that the growth rate of CNTs at eutectic temperature (Fe-C phase diagram for thin films) is higher in comparison with other temperatures [17]. For thin films of iron the eutectic temperature is around 732 ºC [18].

3.3. Raman spectroscopy

Raman Spectroscopy (**Figure 3**) can be used to evaluate the quality of the CNTs by studying the different modes of the spectrum such as D band (1330-1360 cm^{-1}) which is related to the structure disorder due to the presence of amorphous carbon, G band (1550-1600 cm^{-1}) related to the tangential vibration of the carbon atoms. The ratio between D and G bands intensities I_D / I_G evaluates the defects extension within CNTs and it increases as defects increase [13, 19, 20]. This ratio was quite similar for the four samples which means that the temperature change does not affect strongly on the number of defects.

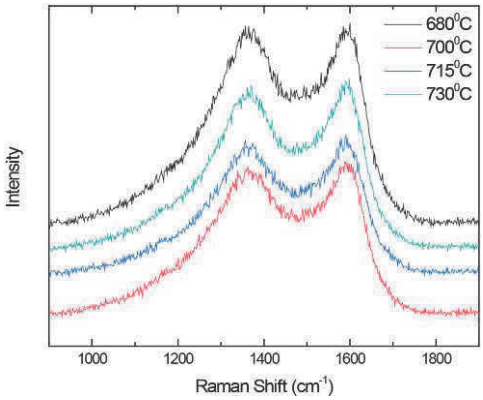

Figure 3 Raman spectrum of CNTs samples

4. CONCLUSION

The thermal stability of AlN/G-SS304 at high annealing temperatures was successful. The G-SS304 acts as a buffer layer between AlN and SS304 foil. Hence, this nitrided layer allows the formation of iron nanoislands on AlN layers and consequently the growth of CNTs. The coalescence phenomenon and the eutectic temperature are important aspects which must be considered to control the morphology of CNTs. However, the use of different growth temperatures does not affect strongly on the number of defects of CNTs. This alternative methodology represents for us a simplified way of obtaining CNTs on stainless steel. We have reduced the time to obtain these nanostructures because we use less targets to obtain an efficient multilayer system for the growth of CNTs.

ACKNOWLEDGEMENTS

The authors acknowledge the financial support of the Spanish Ministry of Economy and Competitiveness under the project ENE2014-56109-C3-1-R, as well as AGAUR (Generalitat de Catalunya) under the project 2014SGR984., Islam Alshaikh and Fernando Pantoja-Suárez acknowledge financial support of their PhD studies to MECD of Spanish Government and to SENESCYT of the Ecuadorian Government, which provided financial support through its scholarship program for 2014, respectively.

REFERENCES

[1] ALRESHEEDI, F.I., KRZANOWSKI, J.E. Structure and morphology of stainless steel coatings sputter-deposited in a nitrogen/argon atmosphere. *Surface & Coatings Technology*, 2017, vol. 314, pp. 105-112.

[2] YANG, X., WANG, X., LING, X., WANG, D. Enhanced mechanical behaviors of gradient nano-grained austenite stainless steel by means of ultrasonic impact treatment. *Results in Physics,* 2017, vol. 7, pp. 1412-1421.

[3] BOGACZ, W., LEMANOWICZ, M., AL-RASHED, M.H., NAKONIECZNY, D., PIOTROWSKI, T., WÓJCIK, J. Impact of roughness, wettability and hydrodynamic conditions on the incrustation on stainless steel surfaces. *Applied Thermal Engineering,* 2017, vol. 112, pp. 352-361.

[4] LEPRO, X., LIMA, M.D., BAUGHMAN, R.H. Spinnable carbon nanotube forests grown on thin, flexible metallic substrates. *Carbon*, 2010, vol. 48, pp. 3621-3627.

[5] ROMERO, P., ORO, R., CAMPOS, M., TORRALBA, J., GUZMAN DE VILLORIA, R. Simultaneous synthesis of vertically aligned carbon nanotubes and amorphous carbon thin films on stainless steel. *Carbon*, 2015, vol. 82, pp. 31-38.

[6] SAKER, A., LEROY, C., MICHEL, H., FRANTZ, C. Properties of sputtered stainless-steel coatings and structural analogy with low temperature plasma nitride layers of austenitic steels. *Materials Science and Engineering: A,* 1991, vol. 140, pp. 702-708.

[7] TERWAGNE, G., HODY, H., COLAUX, J. Structural and quantitative analysis of stainless steel coatings deposited by DC-magnetron sputtering in a reactive atmosphere. *Surface and Coatings Technology*, 2003, vol. 174-175, pp. 383-388.

[8] KAPPAGANTHU, S.R., SUN, Y. Formation of an MN-type cubic nitride phase in reactively sputtered stainless steel-nitrogen films. *Journal of Crystal Growth,* 2004, vol. 267, no. 1-2, pp. 385-393.

[9] KAPPAGANTHU, S.R., SUN, Y. Influence of sputter deposition conditions on phase evolution in nitrogen-doped stainless steel films. *Surface and Coatings Technology*, 2005, vol. 198, no. 1-3, pp. 59-63.

[10] BARANOWSKA, J., FRYSKA, S., SUSZKO, T. The influence of temperature and nitrogen pressure on S-phase coatings deposition by reactive magnetron sputtering. *Vacuum,* 2013, vol.90, pp. 160-164.

[11] DE LOS ARCOS, T., WU, Z.M., OELHAFEN, P. Is aluminum a suitable buffer layer for carbon nanotube growth? *Chemical Physics Letters,* 2003, vol. 380, no. 3-4, pp. 419-423.

[12] NICOLET, M.A. Diffusion barriers in thin films. *Thin solid films*, 1978, vol. 52, pp. 415-443.

[13] MORENO, H.A., HUSSAIN, S., AMADE, R., BERTRAN, E. Growth and functionalization of CNTs on stainless steel electrodes for supercapacitor applications. *Material Research Express,* 2014, vol. 1, pp. 35-50.

[14] HUSSAIN, S., AMADE, R., BERTRAN, E. Study of CNTs structural evolution during water assisted growth and transfer methodology for electrochemical applications. *Materials Chemistry and Physics,* 2014, vol. 148, pp. 914-922.

[15] MOREIRA, M.A., DOI, I., SOUZA, J.F., DINIZ, J.A. Electrical characterization and morphological properties of AlN films prepared by dc reactive magnetron sputtering. *Microelectronic Engineering*, 2011, vol. 88, pp. 802-806.

[16] SIGNORE, M.A., RIZZO, A., ROSSI, R., PISCOPIELLO, E., DI LUCCIO, T., CAPODIECI, L., DIKONIMOS, T., GIORGI, R. Role of iron catalyst particles density in the growth of forest-like carbon nanotubes. *Diamond and Related Materials*, 2008, vol. 17, pp. 1936-1942.

[17] GRÜNEIS, A., KRAMBERGER, C., GRIMM, D., GEMMING, T., RÜMMELI, M.H., BARREIRO, A., AYALA, P., PICHLER, T., SCHAMAN, CH., KUZMANY, H., SCHUMANN, J., BÜCHNER, B. Eutectic limit for the growth of carbon nanotubes from a thin iron film by chemical vapor deposition of cyclohexane. *Chemical Physics Letters*, 2006, vol. 425, pp. 301-305.

[18] HARUTYUNYAN, A.R., TOKUNE, T., MORA, E. Liquid as a required catalyst phase for carbon single-walled nanotube growth. *Applied Physics Letters*, 2005, vol. 87, 051919

[19] Dresselhaus M.S., Dresselhaus G., Saito R. Jorio A. Raman spectroscopy of Carbon Nanotubes, *Physics Reports*, 2008, vol. 409, pp. 47-99.

[20] Osswald S., Havel M., Gogotsi Y. Monitoring oxidation of Multiwalled Carbon nanotubes by Raman Spectroscopy, *Journal of Raman Spectroscopy*, 2007, vol. 38, pp. 728-736.